



# Quasi-classical rate constants for the inelastic process

## $O_2(v_i \gg 1) + O_2 \rightarrow O_2(v_f) + O_2$

JOSE CAMPOS-MARTINEZ<sup>1\*</sup>, ESTELA CARMONA-NOVILLO<sup>1</sup>, JULIAN ECHAVE<sup>2</sup>, MARTA I. HERNANDEZ<sup>1</sup> and JULIANA PALMA<sup>2†</sup>

<sup>1</sup> Instituto de Matemáticas y Física Fundamental (C.S.I.C.), Serrano 123, E-28006-Madrid, Spain

<sup>2</sup> Centro de Estudios e Investigaciones, Universidad Nacional de Quilmes, Sáenz Peña 180, Bernal, Argentina

(Received 7 January 2000; revised version accepted 13 April 2000)

Rate constants have been calculated using quasi-classical trajectories (QCT) for the vibrational relaxation of highly excited  $O_2$ :  $O_2(X^3\Sigma_g^-, v_i) + O_2(X^3\Sigma_g^-, 0) \rightarrow O_2(X^3\Sigma_g^-, v_f) + O_2(X^3\Sigma_g^-)$ , with  $22 \leq v_i \leq 28$ . The present full-dimensional QCT results agree very well with recent quantum reduced dimensionality calculations, giving further support to the hypothesis that the observed experimental jump in depletion rates would be due partially to enhanced vibrational relaxation.

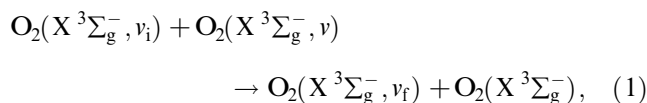
### 1. Introduction

In recent stimulated emission pumping (SEP) experiments Wodtke and coworkers [1, 2] found that the depletion rates of  $O_2(v \gg 1)$  due to collisions with  $O_2(v=0)$  present a jump for a critical value of  $v = v_c$ , where  $v_c$  depends slightly on temperature (for  $T = 295K$ ,  $v_c = 25-26$ , while for  $T = 465K$ ,  $v_c = 26-27$ ). To explain these results, they proposed that the jump was produced by the opening of the reactive channel  $O_2 + O_2 \rightarrow O_3 + O$ . This suggestion was supported by indirect experimental evidence, since there was not a direct ozone detection. This hypothesis was supported also by previous theoretical studies on relaxation rate constants [3, 4] since they showed excellent agreement with experimental data up to initial vibrational excitations close to the mentioned level  $v_c$ . However, all the theoretical studies performed so far [5–8], found that this reaction would be too slow to account for the experimental results of a sharp increase in depletion rates. Recently it has been suggested [9–11] that the jump could be due partially to an enhancement in the vibrational relaxation rates when the system samples the region of the reaction transition state. This suggestion was supported by quantum calculations performed using a reduced dimensionality (RD) model, that considers explicitly only two degrees of freedom. An

inelastic analogue of transition state theory (inelastic transition state, ITS) was proposed [9] to obtain the relaxation rates. However, this ITS has not yet been checked thoroughly. Therefore, although a comparison with experiment was really appealing, further studies are necessary to assert the previous statement.

An exact quantum mechanical (QM) treatment for this system is not possible due to the large masses of the molecules involved. Due to the significance of this system in atmospheric processes and its close relation with the so-called ‘ozone deficit’ problem [12] it is worth exploring other possible treatments that could help us understand the dynamic features of these processes. A practical alternative is to use quasi-classical trajectories (QCT). The QCT method can readily treat the dynamics of the system in its full dimensionality. QCT calculations are inexpensive in terms of memory requirements, compared with QM, and scale very mildly with the number of degrees of freedom. Besides, the large masses and the high vibrational levels (i.e. smaller level spacing) involved make this system specially suited to the QCT approach.

In this work we present the results of a QCT calculation of the rate constants for the inelastic process



where  $v$  is the initial vibrational quantum number of one of the colliding partners, which is always set equal to zero,  $v_i \gg 1$  is the vibrational quantum number being

\* Author for correspondence. e-mail: jcm@imaff.cfmac.csic.es

† Present address: Department of Chemistry, University College London, 20 Gordon St., London WC1H 0AJ, UK.

selected at the beginning of each trajectory and  $v_f$  is the vibrational quantum number assigned at the end of the trajectory. In order to estimate the quality of the QCT approach for this process, we also perform reduced dimensionality QCT calculations, and we compare them with previous quantum results obtained for the same Hamiltonian.

## 2. Calculations

We have calculated full-dimensional rate constants (QCT-FD) which can be compared directly with experimental results. First, an exhaustive convergence check has been made in order to assure the statistical significance of our results. Then in a second step we have also calculated reduced dimensionality probabilities (QCT-RD). These probabilities can be compared directly with the quantum ones (QM-RD), allowing us to assess the validity of the QCT approach for this process, and to check for the adequacy of different quantization procedures. Finally, a comparison between QCT-FD and QM-RD rate constants gives an indication of the accuracy of the ITS approximation used to turn QM-RD probabilities into rate constants, thus confirming our previous statement [9, 10] of an enhanced vibrational relaxation mechanism due to the presence of the reaction channel. In the following sections we give some details about the implementation of the QCT-FD and QCT-RD calculations.

### 2.1. QCT-FD calculations

The FD calculations were performed on the potential energy surface developed by Varandas and Pais [13]. Most of the calculations were done using standard QCT techniques [14]. To simulate the experimental conditions we determined vibrationally state-selected rotationally averaged thermal rate constants. That is, at the beginning of each trajectory the rotational quantum numbers were selected at random from their Boltzmann distributions while the vibrational numbers  $v_i$  and  $v$  were given fixed values for the whole calculation.

The initial conditions for the  $O_2(v=0)$  molecule were obtained from the prescriptions for a rotating Morse oscillator [15]. However, that procedure is not appropriate for the  $O_2(v_i)$  molecule as were interested in high values of  $v_i$ . In this case the correct energy levels can be obtained by applying the EBK quantization rules

$$J = \frac{1}{2\pi} \oint \left( 2\mu(E - V(r)) - \frac{j(j+1)\hbar^2}{r^2} \right)^{1/2} dr = (v + 1/2)\hbar, \quad (2)$$

where  $E$  is the energy of the oscillator,  $j$  is the rotational quantum number,  $v$  is an integer between

zero and infinity, and  $V(r)$  is the actual potential, rather than an approximation suitable only for the lowest levels.

We recently developed an analytical Fourier transform (AFT) method of semiclassical quantization [16], that makes possible the determination of the value of  $v$  corresponding to a given pair  $\{E, j\}$  from equation (2). The procedure can be used to obtain the semiclassical energy levels by iteratively changing  $E$  until an integer value of  $v$  is obtained. For the present case that procedure is quite tedious since, at the temperatures being considered, we have more than fifty rotational numbers for each  $v$ . Therefore, to perform calculations for  $22 \leq v \leq 28$  we should need to repeat the iterative procedure more than 350 times in order to obtain all the possible initial levels.

To overcome this problem, we used the AFT method to build a table with the values of  $E$  for arbitrary values of  $v$  between 21 and 29, and  $j$  between 0 and 76. The table was then used in the trajectory calculations to determine the initial and final states of the excited molecule. At the beginning of each trajectory  $v_i$  and  $j_i$  are known, and the initial energy is obtained by interpolating the values of  $E_i = E(v_i, j_i)$  from the table. At the end of each trajectory both the energy and angular momentum of the diatomic are calculated, and the table is used to obtain  $v_f = v(E_f, j_f)$ . Then, the trajectories are classified as elastic/inelastic. A trajectory was considered inelastic when  $|\Delta v| = |v_f - v_i| \geq 1$ , that is, when the energy transferred in the collision is equal to or greater than the quantum of energy separating the adjacent levels.

The initial collisional energies were selected from a thermal distribution between  $[E_{\min} - \infty)$  using the standard formulae [14]. The impact parameter was selected from a uniform distribution between  $[0 - b_{\max}]$ . The values of  $E_{\min}$  for each vibrational number  $v_i$  were determined from the analysis of full-dimensional reaction probabilities for a zero-impact parameter. The values of  $b_{\max}$  were determined from an analysis of the opacity functions. We checked that the rate constants were converged with respect to small changes of these parameters. For each  $v_i$  we ran  $N_{\text{set}}$  batches of  $N_{\text{traj}}$  trajectories. In order to improve the statistics of the calculations, the generator of random numbers was re-initiated for each batch using a different seed number. The convergence of the rate constants with respect to the total number of trajectories,  $N_{\text{set}} \times N_{\text{traj}}$ , was also studied. The rate constants obtained in this way were multiplied by an electronic factor  $f_{\text{elec}} = 1/3$  to take into account that only three of the nine degenerate electronic states of the reactants correlate with the products.

Table 1. Parameters used in the FD-QCT calculations.

| $v_i$ | $b_{\max}/a_0^2$ | $E_{\min}/eV$ | $N_{\text{set}}$ | $N_{\text{traj}}(295K)$ | $N_{\text{traj}}(465K)$ |
|-------|------------------|---------------|------------------|-------------------------|-------------------------|
| 22    | 4.9              | 0.08          | 10               | —                       | 1000                    |
| 23    | 5.3              | 0.08          | 10               | 2000                    | 1000                    |
| 24    | 5.9              | 0.08          | 10               | 2000                    | 500                     |
| 25    | 7.3              | 0.06          | 10               | 1000                    | 500                     |
| 26    | 7.3              | 0.04          | 10               | 1000                    | 400                     |
| 27    | 7.3              | 0.04          | 10               | 500                     | 400                     |
| 28    | 7.5              | 0.00          | 10               | 500                     | 400                     |

### 2.2. QCT-RD calculations

The reduced dimensionality model we used is the same as that used in the previous quantum studies of process (1) [9, 10]. It considers only two degrees of freedom: the bond length  $r$  for the excited O<sub>2</sub> molecule and the intermolecular distance  $R$ . The bond length of the other O<sub>2</sub> molecule is kept fixed at  $2.35 a_0$  and the orientation of the molecules is the one that minimizes the potential energy for the given values of  $r$  and  $R$ .

The Hamiltonian for this model is given by

$$H = -\frac{\hbar^2}{2\mu} \frac{\partial^2}{\partial R^2} - \frac{\hbar^2}{2\mu} \frac{\partial^2}{\partial r'^2} + V(r', R'),$$

where  $r'$  and  $R'$  are mass-scaled Jacobi coordinates

$$r' = (\mu_r/\mu)^{1/2} r,$$

$$R' = (\mu_R/\mu)^{1/2} R,$$

with  $\mu_r = m_{\text{O}}m_{\text{O}}/(m_{\text{O}} + m_{\text{O}})$ ,  $\mu_R = 2m_{\text{O}}2m_{\text{O}}/(2m_{\text{O}} + 2m_{\text{O}})$  and  $\mu = (\mu_r\mu_R)^{1/2}$ . The reduced dimensionality potential,  $V(r', R')$ , was obtained from the Varandas and Pais potential following the procedure described in detail in [10].

In this case also, standard QCT techniques were used to perform the calculations. Again, the initial and final states of the excited O<sub>2</sub> molecule were determined with the AFT method. The quantization formula for this case can be obtained from equation (2) by setting  $j = 0$ . Therefore, at the beginning of each trajectory we use  $E_i = E(v_i)$  to obtain the initial internal energy of the excited molecule while, at the end of the trajectory, we applied  $v_f = v(E_f)$  to get the final vibrational quantum number. A trajectory was considered inelastic when  $|\Delta v| = |v_f - v_i| \geq 1$ .

### 2.3. Numerical details

Table 1 gives the numerical values of the parameters mentioned in section 2.1 as used for the calculations presented here. As can be seen, more trajectories were run when the probabilities for inelastic collisions were smaller. In order to check the convergence with respect to the total number of trajectories, we determined the

Table 2. Eigenvalues for O<sub>2</sub>( $v_i$ ), obtained with the reduced dimensionality Hamiltonian (QM, quantum; AFT, semiclassical obtained with the AFT method; and Morse, semiclassical corresponding to a Morse oscillator). The parameters of the Morse potential were fitted to give the correct value for the ground state.

| $v_i$ | $E_{\text{QM}}/eV$ | $E_{\text{AFT}}/eV$ | $E_{\text{Morse}}$ |
|-------|--------------------|---------------------|--------------------|
| 22    | 3.675              | 3.674               | 3.679              |
| 23    | 3.789              | 3.796               | 3.801              |
| 24    | 3.905              | 3.914               | 3.929              |
| 25    | 4.019              | 4.027               | 4.048              |
| 26    | 4.118              | 4.136               | 4.165              |
| 27    | 4.233              | 4.240               | 4.279              |
| 28    | 4.333              | 4.340               | 4.389              |

rate constants at intermediate steps during the calculation. After adding a new batch of trajectories, an intermediate rate constant was calculated with the results obtained until that moment. The rate constant obtained after adding the last batch, multiplied by  $f_{\text{elec}}$ , is the final result of the calculation. In figure 1 we show the intermediate rate constants as a function of the number of batches considered. It can be seen that all the rate constants are reasonably well converged after the sixth or seventh batch.

For all the QCT-RD calculations we ran 500 trajectories divided in batches of 50. To show the accuracy achieved with the AFT method, in table 2 we compare quantum and semiclassical AFT vibrational eigenvalues for the O<sub>2</sub> molecule, as obtained with the RD model.

## 3. Results and discussion

Figure 2 compares quantum and QCT inelastic probabilities for the RD model, for two different values of  $v_i$ . We can see that the QCT probabilities describe the threshold behaviour well, up to about 0.25–0.30 eV. However, at higher energies, they underestimate the quantum probabilities. The disagreement found at high energies could be due to a failure of classical mechanics to describe process 1. However, this seems rather unlikely because of the large masses and high quantum numbers involved. Also, the disagreement could be due to the limitations of QCT to deal with state-to-state dynamics. In general, at the end of a trajectory, the final quantum number is non-integer and some criterion must be used to determine if the trajectory is inelastic or not. Although many different ways to assess final quantum numbers in QCT have been proposed and implemented, it was not possible to find a method that was optimal for all the situations. The criterion we followed yields good behaviour of the QCT probabilities at energies near threshold. As the rate con-

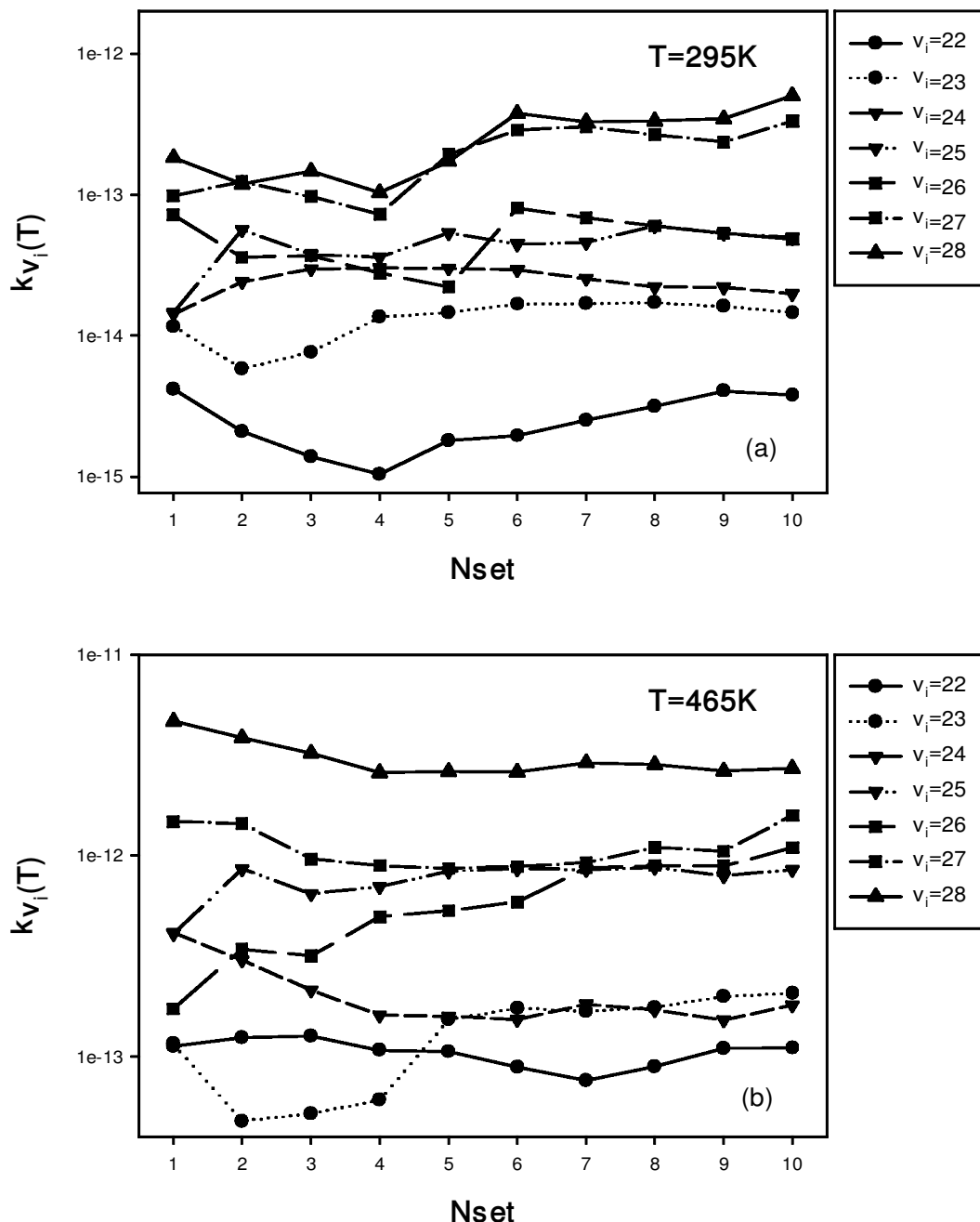


Figure 1. Depletion rate constants for  $\text{O}_2(v_i)$  (a) at  $T = 295\text{ K}$  and (b) at  $T = 465\text{ K}$ , for several  $v_i$  values, as a function of the number of batches of trajectories included in the calculation. The number of trajectories per batch for each  $v_i$  is given in table 1.

stants at the temperatures we are considering are determined by this threshold behaviour, we considered it a good criterion and we also use it for the QCT-FD calculations.

Figure 3 presents the QCT-FD rate constants for  $T = 295\text{ K}$  and  $465\text{ K}$  along with experimental [1, 2], QM-RD [9, 10] and semiclassical results [11]. For  $T = 295\text{ K}$  (figure 3(a)), it can be seen that the QCT-

FD rate constants follow the experimental curve quite well, showing a jump for  $v_i > 26$ . Very good agreement is also found between QCT-FD and QM-RD for  $v_i = 23$ – $26$ . For  $v_i > 26$ , QCT-FD calculations show a jump in the rate constants that is more pronounced than that predicted by the QM-RD calculations, in better agreement with experiment. Nevertheless, QCT-FD values are still below the experimental ones. At

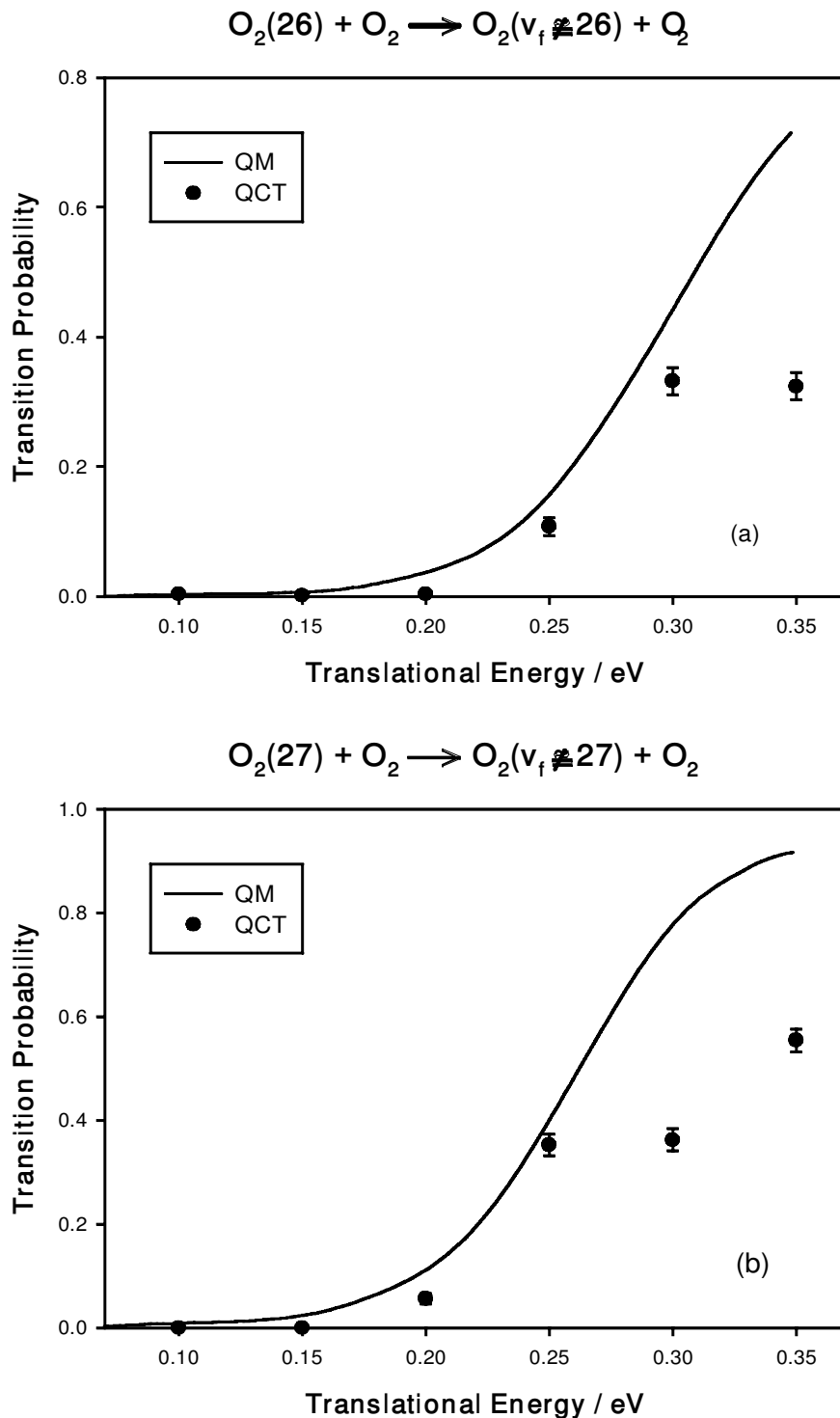


Figure 2. Initial state selected inelastic transition probabilities out of (a)  $v_i = 26$  and (b)  $v_i = 27$  to any final state, as a function of translational energy (in eV). Both QCT (points with error bars) and quantum calculations (lines) are performed using the same reduced dimensionality model [10].

$T = 465$  K (figure 3(b)), the QCT-FD rate constants compare quite well with the QM-RD, and remarkably well with the semiclassical calculation of Balakrishnan *et al.* [11] for the range  $v_i = 25$ –28. However, all treatments give an increase in the rate constants as functions of  $v_i$  smoother than found in the experiments. In addition,

the strongest increase occurs at a value of  $v_i$  smaller than that of the measurements. The strongest increase occurs at  $v_i = 24$ –25 for QCT, while in the experiments it appears at  $v_i = 27$ –28.

Therefore, the present full-dimensional QCT calculations agree with the QM-RD of [9, 10] in predicting that

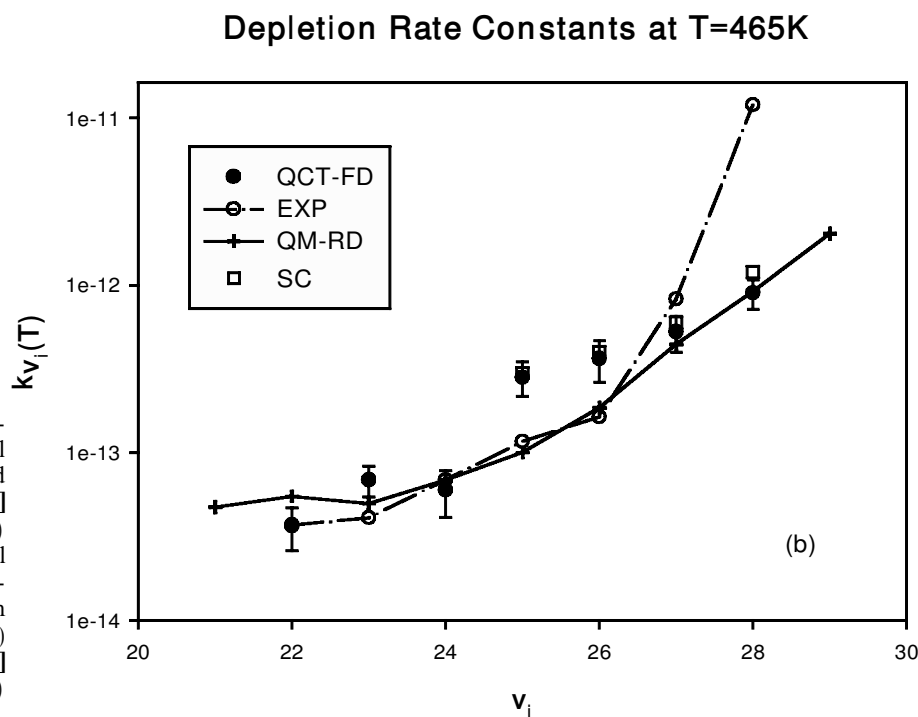
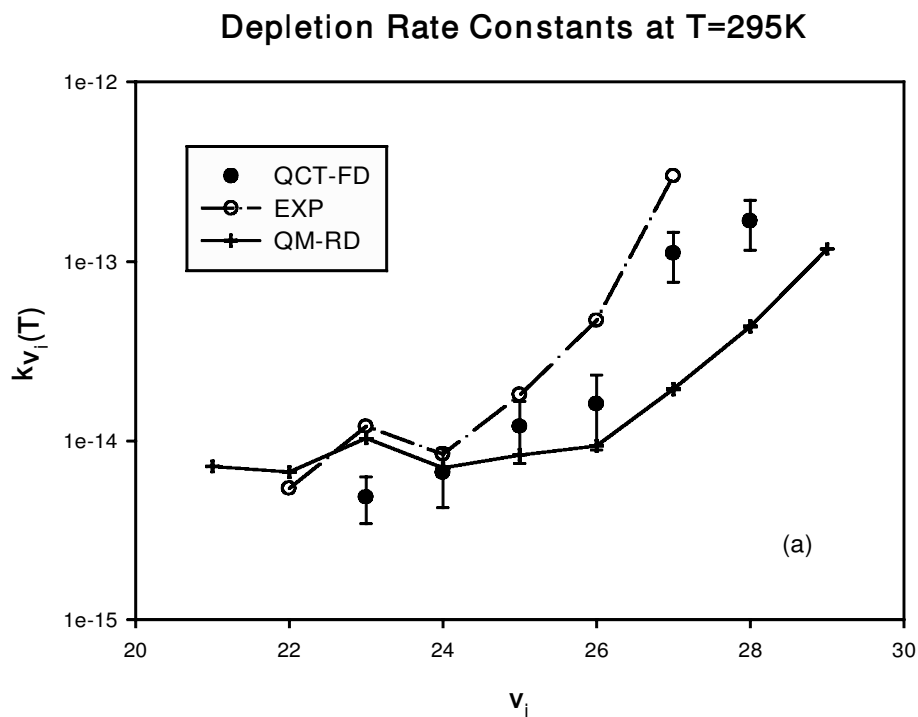


Figure 3. (a) Full-dimensional quasiclassical (QCT-FD), experimental (EXP) [1, 2] and quantum reduced dimensionality (QM-RD) [9, 10] depletion rate constants for  $O_2(v_i)$  at  $T = 295$  K. (b) Full-dimensional quasiclassical (QCT-FD), experimental (EXP) [1, 2], quantum reduced dimensionality (QM-RD) [9, 10] and semiclassical (SC) [11] depletion rate constants for  $O_2(v_i)$  at  $T = 465$  K.

the jump in the rate constants can be explained partially by vibrational relaxation. This qualitative agreement is remarkable, taking into account that each of these calculations involve several approximations, and that the nature of the approximations used in

each case are very different, and independent of each other. As discussed in detail in those references, the use of a PES exhibiting the reactive channel is the origin of the jump in the relaxation rates. For a sufficiently high initial vibrational level, the region in the

PES near the reaction transition state is sampled, and therefore although reaction occurs with a very small probability an energy transfer is favoured leading to an enhancement of the inelastic process.

On the other hand, it has to be noted that there are still important differences between the predictions of the calculations and the experimental results, especially at  $T = 465$  K. Several reasons could explain these differences. Some time ago, it was suggested that the Varandas and Pais surface did not describe accurately the O<sub>2</sub> + O<sub>2</sub> channel [17]. More interestingly there have been several suggestions on other possible mechanisms that could help us understand this jump in relaxation rate constant, such as the existence of a four-centre reaction mechanism on the singlet surface [8], and much more recently it has been proposed that electronic non-adiabatic effects could play an important role in O<sub>2</sub>( $v_i \gg 1$ ) + O<sub>2</sub>( $v = 0$ ) collisions [18]. These non-adiabatic processes could have important implications for the understanding of the mechanisms of O<sub>2</sub> in the upper atmosphere.

#### 4. Conclusion

We have presented full-dimensional QCT rate constants for the inelastic process O<sub>2</sub>(X<sup>3</sup>Σ<sub>g</sub><sup>-</sup>,  $v_i$ ) + O<sub>2</sub>(X<sup>3</sup>Σ<sub>g</sub><sup>-</sup>,  $v$ ) → O<sub>2</sub>(X<sup>3</sup>Σ<sub>g</sub><sup>-</sup>,  $v_f$ ) + O<sub>2</sub>(X<sup>3</sup>Σ<sub>g</sub><sup>-</sup>). These QCT calculations agree well with previous quantum mechanical calculations in which a reduced dimensionality model together with a new approximate method for calculating inelastic rate constants was introduced. From the comparison, we can say that our RD model plus inelastic transition state proposition provides us with reasonable and sensible results for rate constants, also confirmed by semiclassical calculations [11]. Thus, all the calculations indicate an increase in the rate constants after a critical value of  $v_i$  that can be explained by enhanced vibrational relaxation. However, there are still differences between calculated and experimental rate constants that will possibly need some refinement of the available PES as well as more studies on alternative mechanisms probably involving more than one electronic surface.

This work has been supported partially by the DGICYT (Spain), Grant Number PB95-0071, and the EU, Contract FMRX-CT96-0088.

#### References

- [1] PRICE, J. M., MACK, J. A., ROGASKI, C. A., and WODTKE, A. M., 1993, *Chem. Phys.*, **175**, 83.
- [2] ROGASKI, C. A., MACK, J. A., and WODTKE, A. M., 1995, *Faraday Discuss. chem. Soc.*, **100**, 229.
- [3] BILLING, G. D., and KOLESNICK, R. E., 1992, *Chem. Phys. Lett.*, **200**, 382.
- [4] HERNÁNDEZ, R., TOUMI, R., and CLARY, D. C., 1995, *J. chem. Phys.*, **102**, 9544.
- [5] BALAKRISHNAN, N., and BILLING, D. G., 1995, *Chem. Phys. Lett.*, **242**, 68.
- [6] HERNÁNDEZ-LAMONEDA, R., HERNÁNDEZ, M. I., CARMONA-NOVILLO, E., CAMPOS-MARTÍNEZ, J., ECHAVE, J., and CLARY, D. C., 1997, *Chem. Phys. Lett.*, **276**, 152.
- [7] VARANDAS, A. J. C., and WANG, W., 1997, *Chem. Phys. Lett.*, **215**, 167.
- [8] LAUVERGNAT, D. M., and CLARY, D. C., 1998, *J. chem. Phys.*, **108**, 3566.
- [9] CAMPOS-MARTÍNEZ, J., CARMONA-NOVILLO, E., ECHAVE, J., HERNÁNDEZ, M. I., HERNÁNDEZ-LAMONEDA, R., and PALMA, J., 1998, *Chem. Phys. Lett.*, **289**, 150.
- [10] CAMPOS-MARTÍNEZ, J., CARMONA-NOVILLO, E., ECHAVE, J., HERNÁNDEZ, M. I., HERNÁNDEZ-LAMONEDA, R., and PALMA, J., 1998, *Eur. Phys. D*, **4**, 159.
- [11] BALAKRISHNAN, N., DALGARNO, A., and BILLING, D. G., 1998, *Chem. Phys. Lett.*, **288**, 657.
- [12] ELUSZKIEWICZ, J., and ALLEN, M., 1993, *J. geophys. Res.*, **98**, 1069.
- [13] VARANDAS, A. J. C., and PAIS, A. A. C. C., 1991, *Theoretical and Computational Models for Organic Chemistry* edited by L. C. Arnaut, S. J. Formosinho and I. G. Czismadia (Dordrecht: Kluwer).
- [14] RAFF, L. M., and THOMPSON, D. L., 1985, *The Theory of Chemical Reaction Dynamics*, Vol. 1, edited by M. Baer (Boca Raton, FL: CRC Press).
- [15] PORTER, R. N., RAFF, L. M., and MILLER, W. H., 1975, *J. chem. Phys.*, **63**, 2214.
- [16] PALMA, J., and ECHAVE, J., 1997, *Chem. Phys. Lett.*, **270**, 206.
- [17] MACK, J. A., HUANG, Y., SCHATZ, G. C., and WODTKE, A. M., 1996, *J. chem. Phys.*, **105**, 7495.
- [18] JONGMA, R. T., SHI, S., and WODTKE, A. M., 1999, *J. chem. Phys.*, **111**, 2558.